Experimental investigation on spiked body in hypersonic flow

R. Kalimuthu
Vikram Sarabhai Space Center
Trivandrum, India

R. C. Mehta
Nanyang Technological University
Singapore

E. Rathakrishnan
Indian Institute of Technology
Kanpur, India

ABSTRACT

A spike attached to a hemispherical body drastically changes its flowfield and influences aerodynamic drag in a hypersonic flow. It is, therefore, a potential candidate for drag reduction of a future high-speed vehicle. The effect of the spike length, shape, spike nose configuration and angle-of-attack on the reduction of the drag is experimentally studied with use of hypersonic wind-tunnel at Mach 6. The effects of geometrical parameters of the spike and angle-of-attack on the aerodynamic coefficient are analysed using schlieren picture and measuring aerodynamic forces. These experiments show that the aerodisk is superior to the aerospike. The aerodisk of appropriate length, diameter, and nose configuration may have the capability for the drag reduction. The including of an aero disk at the leading edge of the spike has an advantage for the drag reduction mechanism if it is at an angle-of-attack, however consideration to be given for increased moment resulting from the spike is required.
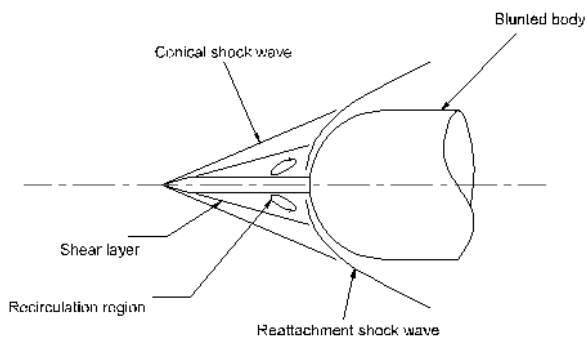
1.0 INTRODUCTION

Investigations into the effects of forward facing spike on hypersonic bodies have been carried out since the late 1940s. The prime concern has been with regard to drag characteristics where effects due to spike length, spike head geometry, forward body geometry and relative spike diameter have been explored. The drag exerted on a body in supersonic and hypersonic flow is an important problem of aerodynamics. For reentry into the Earth's atmosphere, it is important to co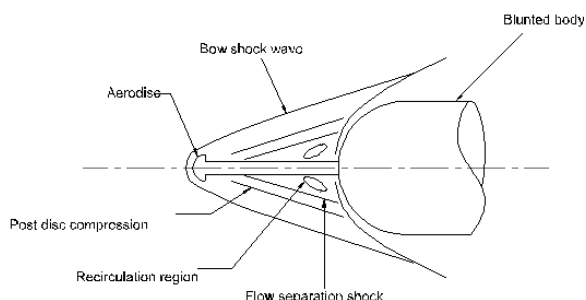ntrol the deceleration of a reentry capsule by harnessing the drag. Conversely, for escape from the atmosphere, the drag on the body should be reduced. Attaching a spike to the nose can reduce the drag on a blunt body.

The aerospike substantially reduces fore-body drag by creating a low dynamic pressure region of separated flow over the high volume nose fairing. The studies of hypersonic drag reduction focused on the use of a structural spike protruding upstream and attached to the blunt body. Many studies have shown that the recirculating regions and the resulting conical shock wave created ahead of a body equipped with a conical spike results in reduced pressure on the body surface, which reduces the overall drag[1,2]. Mehta[3] found in the numerical flow simulations over the conical spike attached to blunted body that in addition to the aerodynamic drag reduction, heat transfer was also reduced as the length of the spike increases. However, spike lengths larger than some critical length were not effective due to the detachment of the shock structure from the point of the spike and its reformation as a strong normal shock just upstream of the body. Another finding of this particular study was that the spike friction on the body itself is reduced due to the presence of the large recirculation regions adjacent to the body nose.
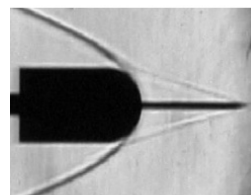
Several experimental studies have been conducted to examine the fore body flow field of the spike blunt body. Most of the experimental investigations conducted in the 1950s concentrated on issues related to high pressures and heating rates around such configurations and possible mechanism to reduce them. Stadler and Nielsen[4] carried out experiments on a hemisphere-cylinder configuration at freestream Mach numbers of 1·5, 2·67, and 5·0, and a Reynolds
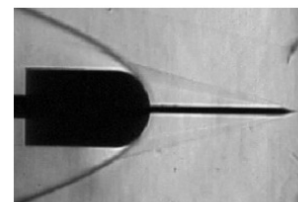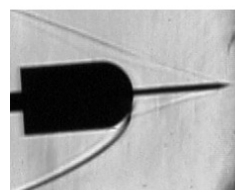
(a) Conical spike

(b) Aerodisc

Figure 1. Schematic sketch for flow field over forward facing spike.

(a) Geometrical detail of the model

(b) Conical Aerospike   (c) Hemisphere Aerodisk

(d) Flat-Face Aerodisk

Figure 2. Dimensions of the spiked blunt body.

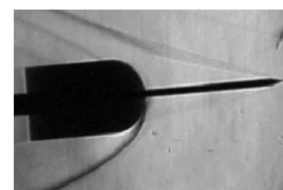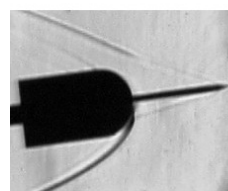$\alpha = 0$ deg $\alpha = 0$ deg

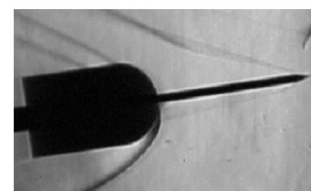$\alpha = 5$ deg $\alpha = 5$ deg
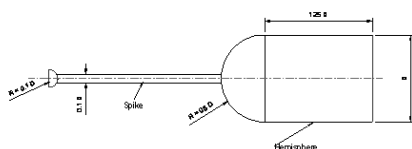
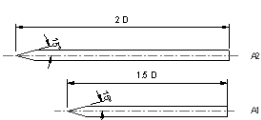$\alpha = 8$ deg $\alpha = 8$ deg

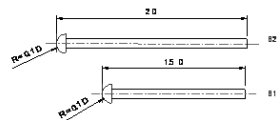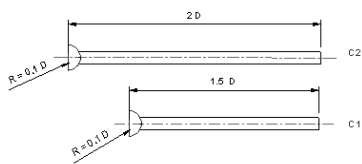$L/D = 1\cdot5$ $L/D = 2\cdot0$

Figure 3. Schlieren pictures for conical spike.

number in the range of $0\cdot16 \times 10^6 - 0\cdot85 \times 10^6$ based on the diameter of the cylinder. Their experiments indicated a reduction in surface pressure and, consequently, the drag, with the attachment of the forward facing spike.

The experimental investigation of Bogdonoff and Vas[5] indicated an initial drop of pressure at the nose of the fore-body with increased spike length up to an L/D ratio of three (where L is the spike length and D is cylinder diameter). Crawford[6] experimentally investigated the effect of the spike on the nature of the flowfield, the surface pressure distribution, and the heat flux variation for a freestream Mach number of 6·8 and Reynolds number of $0\cdot16 \times 10^6 - 0\cdot85 \times 10^6$ based on the diameter of the cylinder. According to his experimental analysis, the drag and the heat flux were reduced when the spike was lengthened, but the spike length did not influence the drag when the latter exceeds the blunt-body diameter by roughly four times.

These experimental investigations provide insight into the characteristics of the separated region created by an adverse pressure gradient and shock/boundary-layer interaction over the blunt nose. Unsteadiness of the flow caused by the spike that the shock wave around the body oscillates when the nose has a plane shape. In 1960, Maull[7] studied unsteadiness of the flow caused by the spike on the blunt body nose. Wood[8] investigated experimentally the flow field over the spiked cone and found that the shape and size of a region of separated flow is controlled primarily by the flow near the reattachment point. Fluctuating pressures in spike-induced flow separation was observed experimentally by Guenther and Reding[9]. The spike is also an effective way to reduce the aerodynamic drag due to the reduced dynamic pressure in the separated flow region.

Motoyama et al[10] have experimentally investigated the aerodynamic and heat transfer characteristics of conical, hemispherical, flat-faced aerospike, and hemispherical and flat-faced disk attached to the aerospike for freestream Mach number 7, freestream Reynolds number 4×10^5/m, for $L/D = 0\cdot5$ and $1\cdot0$, and angle-of-attack 0 to 8 deg. They found that the aerodisk spike ($L/D = 1\cdot0$ and aerodisk
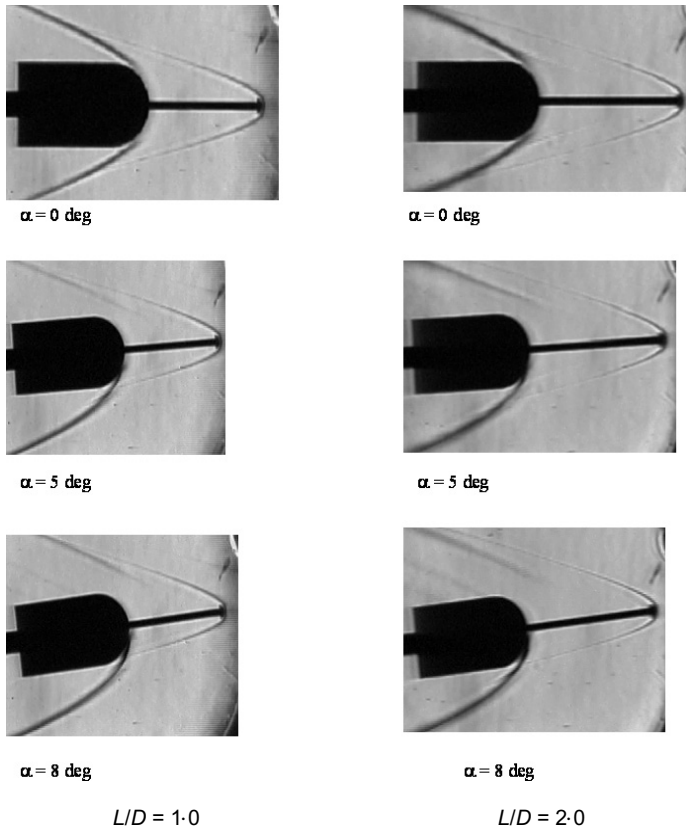
α = 0 deg

α = 5 deg

α = 8 deg

L/D = 1·0   *L/D* = 2·0

Figure 4. Schlieren pictures for hemisphere aerodisk.

α = 0 deg

α = 5 deg

α = 8 deg

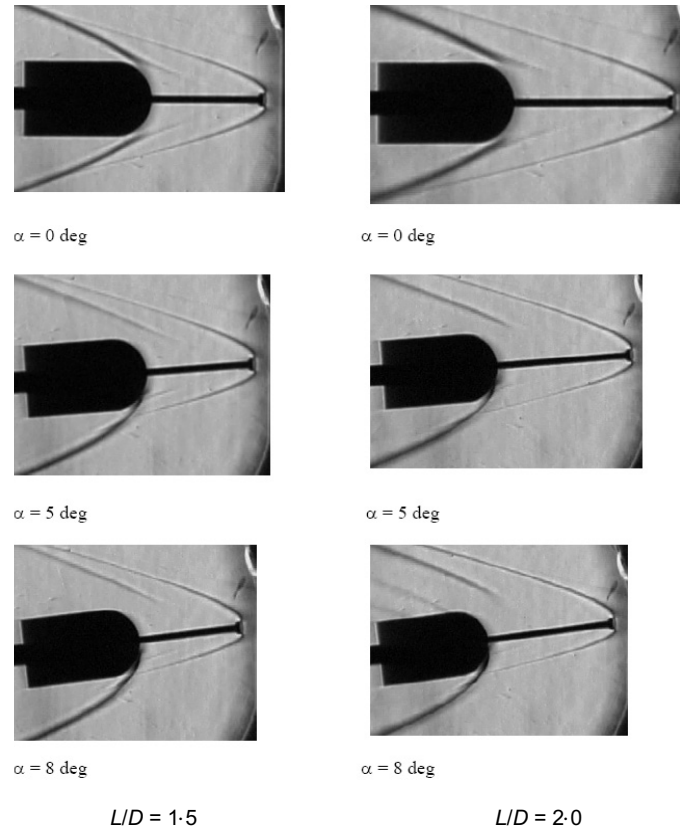*L/D* = 1·5   *L/D* = 2·0

Figure 5. Schlieren pictures for flat-face aerodisk.

diameter of 10mm) has a superior drag reduction capability as compared to the other aerospikes.

Yamauchi *et al*[11] have numerically investigated the flow field around a spiked blunt body at freestream Mach numbers of 2·01, 4·14 and 6·80 for different ratio of *L/D*. The features of the high-speed flow field can be delineated through these experimental investigations. It is characterised by a conical shock wave from the tip of the spike, a reattachment shock wave on the blunt body, and a separated flow region ahead of the blunt body. A schematic of the flow field over the conical and the aerodisk spiked blunt body at zero angle-of-attack is shown in Figs 1(a) and (b), respectively. The flow field around a spiked blunt body appears to be very complicated and complex and contains a number of interesting flow phenomena and characteristics, which have yet to be investigated. A spike drastically influences the aerodynamic drag of the blunted body in hypersonic flow. The recirculating region is formed around the root of the spike up to the reattachment point of the flow at the shoulder of the hemispherical body. Due to the recirculating region, the pressure at the stagnation region of the blunt body will decrease[12]. However, because of the reattachment of the shear layer on the shoulder of the hemispherical body, the pressure near that point becomes large. Whether the reattachment point can be moved backward or removed, depends on the spike length or the nose configuration[13,14]. Milicev *et al*[15] have experimentally investigated the influence of four different types of spikes attached to a hemisphere-cylinder body at Mach number 1·89, Reynolds number $0·38 \times 10^6$ based on the cylinder diameter, and angle-of-attack 2°. They observed in the experimental studies that the reliable estimating of aerodynamic effects of the spike can be made in conjunction with flow visualisation technique. Numerical simulations[16,17] have been performed to get the comparative studies of flowfield features over a payload fairing of a typical satellite launch vehicle with and without forward facing spike for freestream Mach number range $0·9 \leq M_\infty \leq 3·0$ and freestream Reynolds number range of $33·35 \times 10^6/m \leq Re_\infty \leq 46·75 \times 10^6/m$.

Experimental studies were carried out to measure the aerodynamic forces in the presence of the spike attached to the blunt body for the length to diameter ratio of 1·5 and 2·0 and angle-of-attack up to 8°deg at Mach number 6 in the center's hypersonic wind-tunnel. In the present experimental study, the effect of a flat aero disk or a hemispherical aero disk attached to the leading end of the spike is investigated. The flow field visualisation will be made using schlieren pictures with different shape of spike such as conical, hemispherical disk and flat-face spikes. The flow field features captured by the schlieren picture was used to determine the mechanism of the drag reduction. The coefficients of drag, lift and pitching moment were measured for different spike configurations using the six-component strain gauge balance. The influence of the spike shock wave generated from the spike interacts with the reattachment shock were also investigated to understand the cause of drag reduction.

2.0 EXPERIMENT

The hypersonic wind tunnel (HWT) used for this study is an axisymmetric, enclosed free jet tunnel with a free jet diameter of 254mm. This facility is of pressure vacuum type. The tunnel system consists of high pressure air supply, a pebble bed heater, a contoured nozzle for delivering flow of the required Mach number, a free jet test-section, a fixed geometry diffuser with scoop to collect the nozzle flow and the vacuum system. The facility is designed to provide Mach number range of 4 to 8 and Reynolds number 1 to 18 millions (based on free-jet diameter). The facility is equipped with state of the art instrumentation system and required sensors.

2.1 Models

Various spike configurations were tested in this experiment. The dimensions of the spiked blunt body considered in the present work
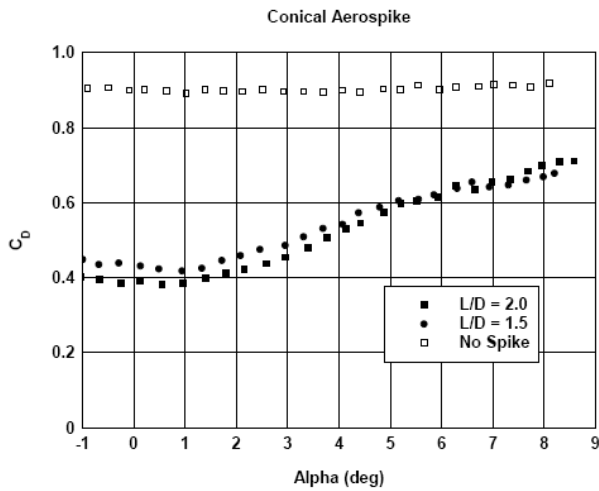
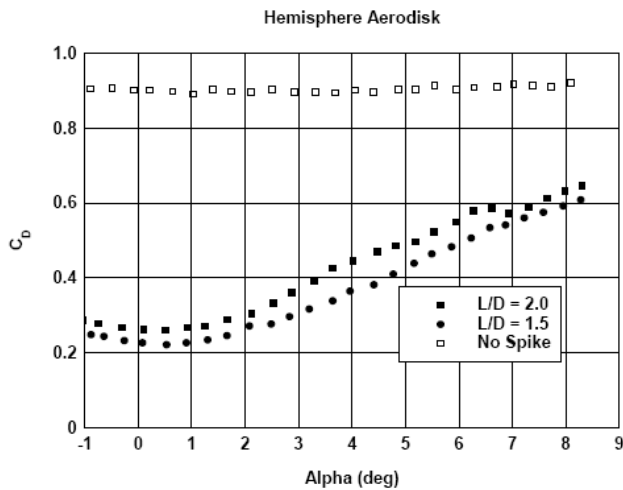Figure 6. Drag coefficient variation for conical aerospike of different *L/D*.

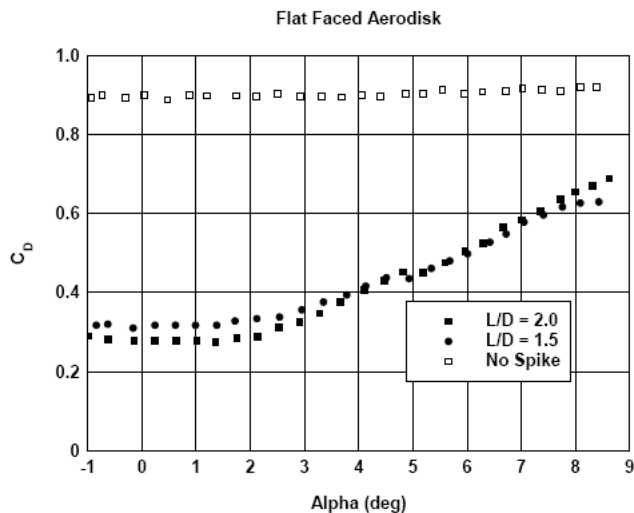Figure 7. Drag coefficient variation for hemisphere aerodisk of different *L/D*.

Figure 8. Drag coefficient variation for flat faced aerodisk of different *L/D*.

are shown in Fig. 2. The model is axisymmetric, the main body has a hemisphere-cylinder nose and D is diameter as shown in Fig. 2(a). The spike consists of a conical part and a cylinder part. The diameter of the cylinder of the spike is $0·1D$. The spike model has a simple stick configuration. The spike lengths L of $1·5$ and $2·0D$ are tested in the experiment.

The angle of the cone is 15°deg for the conical spike as depicted in Fig. 2(b). The aerodisk type spike configuration utilised a disk on its nose of radius $0·1D$ as shown in Fig. 2(c). In other study, the aero flat-face disk is considered and shown in Fig. 2(d). The radius of the aerodisk is $0·05D$. The diameter of the aerodisk attached to the spike is twice that of the diameter of the spike-stem. This can be seen in Figs 2(c) and 2(d).

2.2 Force measurements

Using the six component strain gauge balance, the coefficients of drag, lift and pitching moment are measured for different type of the spike configurations at Mach 6 and $\alpha = 0 – 8$°deg. The D is taken as reference diameter for the calculation of the aerodynamic coefficients.

3.0 RESULTS AND DISCUSSION

3.1 Flowfield visualisation

Figures 3-5 show schlieren photographs of the flowfield around the hemispherical body with the conical aerospike, hemispherical aerodisk and flat-faced aerodisk with $L/D = 1·5$ and $2·0$. The flowfields are very different between the aerospike of conical, hemispherical aerodisk and flat-faced aerodisk as seen in the schlieren pictures.

In the case of the conical spike, the conical shock wave is emanated from the spike nose. The separated shear layer and the recompression shock from the reattachment point on the shoulder of the hemispherical body are visible. Figure 3 shows the effects of L/D ratio and the angle-of-attack on the flowfield. The conical shock wave moves further away from the blunted body as compared to $L/D = 1 × 5$ and $2 × 0$, and the increase of L/D ratio increases the recirculation zone in the windward side with the angle-of-attack.

In the aerodisk case as depicted in Figs 4 and 5, the bow shock wave is emanating far from the hemispherical body. The bow shock wave generated from the aerodisk is affected by the angle-of-attack. The body is completely enveloped within the recirculation region, which is separated from the inviscid flow within the bow shock wave by a separation shock. The bow shock interacts with the reattachment shock generated by the blunt body. The interaction of the shock wave produced by the hemispherical aerospike differs significantly with the conical spike. The flow separation on the spike and recirculation zone formed on the blunt body cap depends on shape of the spike. The schlieren pictures explain the cause of the drag reduction due to increase of the separation region over the aerodisk type of spike. The normal shock in front of the spike cap will reduce the drag as compared without the spike. In the fore region of the aerodisk, the fluid decelerates through the bow shock wave. At the shoulder of the aerodisk or hemispherical cap, the flow turns and expands rapidly, and the boundary layer detaches, forming a free shear layer that separates the inner re-circulating flow region behind the base from the outer flow field. The corner expansion over aero disk process is a modified Prandtl-Mayer pattern distorted by the presence of the approaching boundary layer.

The schlieren pictures reveal the flowfield behavior over the spike and also the drag reduction mechanism due to the interaction of the shock waves, which is influenced by the spike configurations as observed in the schlieren pictures. As the curvature radius of the spike nose becomes large from a conical nose to a flat-faced
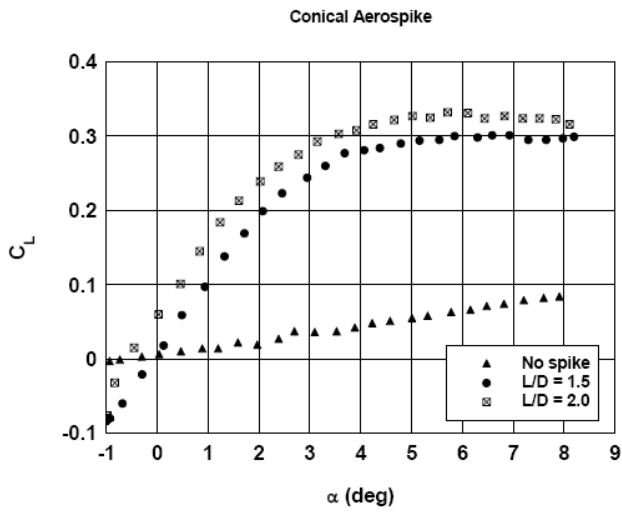
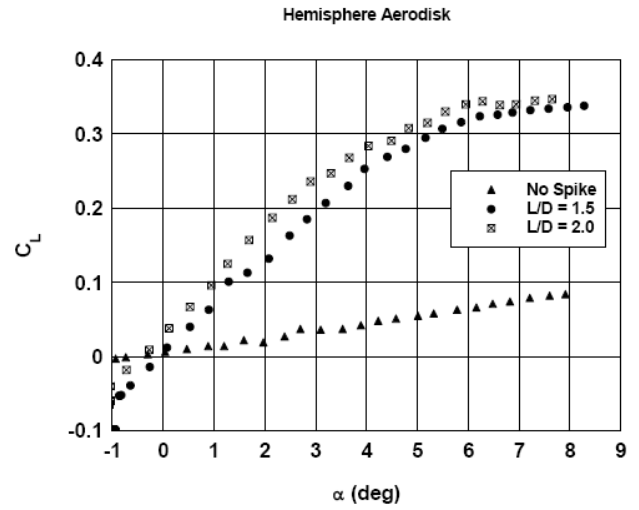Figure 9. Lift coefficient variation for conical aerospike of different *L/D*.

Figure 10. Lift coefficient variation for Hemisphere Aerodisk different *L/D*.
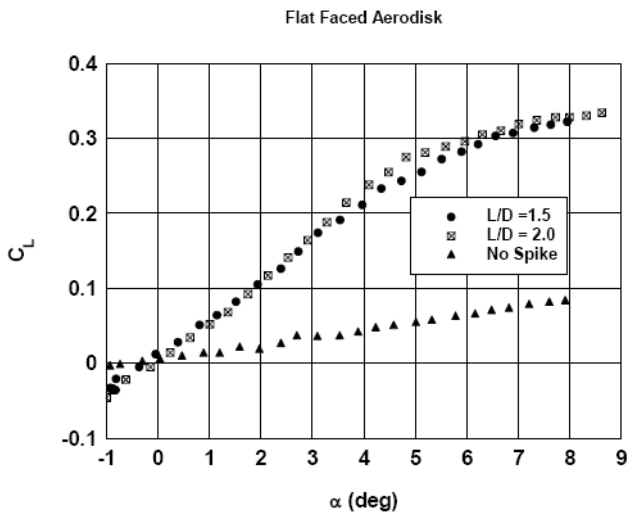

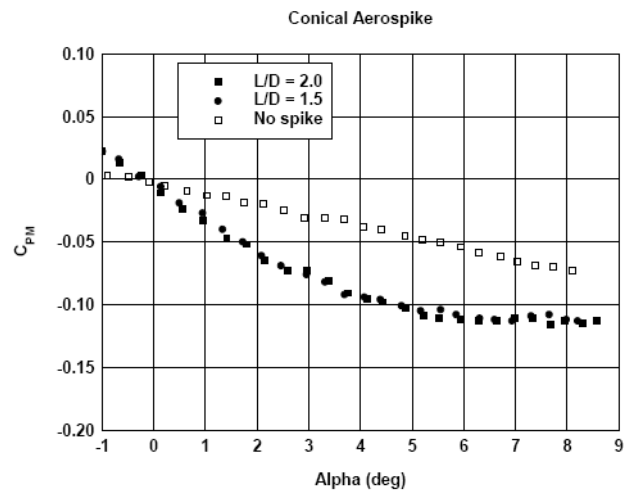Figure 11. Lift coefficient variation for Flat Faced Aerodisk different *L/D*.

Figure 12. Pitching moment coefficient variation
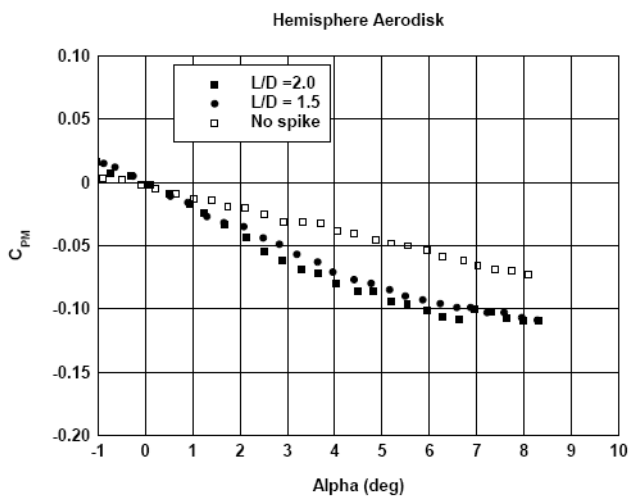for conical aerospike of different *L/D*.

Figure 13. Pitching moment coefficient variation
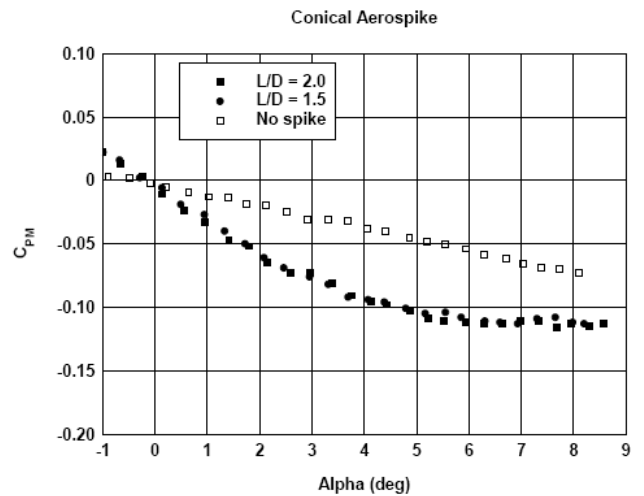for Hemisphere aerodisk of different *L/D*.

Figure 14. Pitching moment coefficient variation
for flat faced aerodisk of different *L/D*.

nose, the total pressure drag decreases. From the flow field point of view, the aerodisk with $L/D = 2·0$ has the potential for the greatest drag reduction in this experiment result. Motoyama et al[10] also experimentally observed through the flow visualisation technique at Mach 7 that a bow shock wave generated ahead of the aerodisk, and a large recirculating zone enveloped the aerodisk spike. It was found by them that the aerodisk spike has shown better drag reduction capability in comparison with other types of the aerospike configurations.

3.2 Aerodynamic effect of spike on angle-of-attack

From sting balance measurements, the drag, the lift and the pitching moment on the body without a spike and with the conical spike, hemispherical disk and flat-faced disk ($L/D = 1·5$ and $2·0$) at angle-of-attack 0 to 8°deg are shown in Figs 6 to 14. Five repeated tests[18] were conducted for the hemisphere aerodisk spike of $L/D = 1·5$ in order to get the repeatability of the measured data. The repeatability tests data were analysed and shown error bands of $±2·4\%$ in lift and drag coefficients. Numerical simulations[3,18] have been made to validate the experimentally measured drag coefficient for the conical aerospike at Mach 6 and zero angle-of-attack. The maximum drag coefficient difference between the experimental and the numerical results is found to be about 7%.

A comparative performance of the drag coefficient, CD can be obtained from Figs 6-8. From these figures, the comparison of the drag on each spiked blunt body configurations (conical, disk and flat-face) at an angle-of-attack of 8°deg can be observed. It is important to note that the spike is advantageous for drag reduction when the spherical body is at an angle-of-attack. This is also observed in the above flowfield visualisations. The drag on a cone is smaller than that on a blunt body without the spike. Thus, the drag is reduced because of the existence of the separated region created by the spike on the nose. With an increase in the angle-of-attack, the separated flow at the nose becomes asymmetric in the pitch plane. The extent of separation reduces on the windward surface and increases on the leeward surface. At angle-of-attack it is most likely that the windward separated flow between the spike and the body nose is swept to the leeward surface and vented via shedding vortices. Figures 9-11 show the variation of the lift coefficient, CL for the conical, hemispherical disk and flat-faced disk shape spikes. The lift coefficient increases with the increase of angle-of-attack. Comparative performance of the pitching moment, CPM on each spike configurations (conical, disk and flat-face) at angle-of-attack up to 8°deg is shown in Figs 12-14. It can be seen from the figures that when the model with a spike is at an angle-of-attack it is subject to a large pitching moment resulting from the spike itself. As the angle-of-attack increases the pitching moment increases more rapidly. Thus, it is important to note that the consideration for compensation of the increased pitching moment is required in order to account the usefulness of the spike in the angle-of-attack situations.

CONCLUSION

Flow observation and six degrees of freedom force measurements on the blunt body with a conical, hemispherical disk and flat-faced spike are carried out at Mach 6 in a hypersonic wind-tunnel. The flow fields show different flow features between the conical spike, the hemispherical aerodisk and the flat-faced aerodisk. The effects of the spike geometrical parameters as well as shape on the drag, the lift and the pitching moment are studied experimentally. A forward facing spike attached to a hemispherical body alters significantly the structure of the flowfield and serves to reduce drag by the formation of a recirculation region around the stagnation point of the blunt body. The flow field, immediately behind the aero disk shows a complex flow field due to back-disk geometry as compared to the conical spike. To take advantage of the forward facing spike for more efficient drag reduction, the reattachment point of the shear layer on the body should be moved backward by choosing the optimal spike length with suitable geometrical configuration of the nose. From the standpoint of drag reduction without considering aerodynamic stability, the aerodisk with $L/D = 2·0$ is most effective among the models tested. Consideration for compensation of the increased pitching moment is needed.

REFERENCES

1. YAMAUCHI, M., FUJII, K. and HIGASHINO, F. Numerical investigation of supersonic flows around a spiked blunt body, *J Spacecraft and Rockets*, 1995, **32**, (1), pp 32-42.
2. HUTT, G.R. and HOWE, A.J. Forward facing spike effects on bodies of different cross section in supersonic flow, *Aeronaut J*, 1989, **93**, (6), pp 229-234.
3. MEHTA, R.C. Numerical heat transfer study over spiked-blunt body at Mach 6.80, AIAA paper 2000-0344, January 2000.
4. STADLER, J.R. and NIELSEN, H.V. Heat transfer from a hemisphere-cylinder equipped with flow-separation spikes, NACA TN 3287, September 1954.
5. BODONOFF, S.N. and VAS, I.E. Preliminary investigations of spiked bodies at hypersonic speeds, *J Aerospace Sciences*, 1959, **26**, (2), pp 65-74.
6. CRAWFORD D.H. Investigation of the flow over a spiked-nose hemisphere cylinder at a Mach number of 6.8, NASA TN D-118, December 1959.
7. MAULL, D.J. Hypersonic flow over axially symmetric spiked bodies, *J Fluid Mechanics*, 1960, **8**, (4), pp 584-592.
8. WOOD, C.J. Hypersonic flow over spiked cones, *J Fluid Mechanics*, 1962, **12**, (4), pp 614-627.
9. GUENTHER, R.A. and REDING, J.P. Fluctuating pressure environment of a drag reduction spike, *J Spacecraft and Rockets*, 1977, **44**, (12), pp 705-710.
10. MOTOYAMA, N., MIHARA, K., MIYAJIMA, R., WATANUKI, T. and KUBOTA, H. Thermal protection and drag reduction with use of spike in hypersonic flow, AIAA paper 2001-1828, April 2001.
11. YAMAUCHI, M., FUJII, K., TAMURA, Y. and HIGASHINO, F. Numerical investigation of supersonic flows around a spiked blunt body, AIAA paper 93-0887, January 1993.
12. FUJITA, M. and KUBOTA, H. Numerical simulation of flow field over a spiked-nose, *Computational Fluid Dynamics J*, 1992, **1**, (2), pp 187-195.
13. REDING, J.P., GUENTHER, R.A. and RICHTER, B.J. Unsteady aerodynamic considerations in the design of a drag-reduction spike, *J Spacecraft and Rockets*, 1970, **14**, (1), pp 54-60.
14. ZEREA, C. and ROM, J. Effects of a spike on the drag and on the aerodynamic stability of blunt bodies in supersonic flow, *J Spacecraft and Rockets*, 1970, **7**, (8), pp 1017-1019.
15. MILICEV, S.S., PAVLOVIC, M.D., RISTIC, S. and VITIC, A. On the influence of spike shape at supersonic flow past blunt bodies, *Mechanics, Automatic Control and Robotics*, 2002, **3**, (12), pp 371-382.
16. MEHTA, R.C. and JAYACHANDRAN, T. Navier-Stokes solution for a heat shield with and without a forward facing spike, *Computers & Fluids*, 1997, **26**, (7), pp 741-754.
17. MEHTA, R.C. Heat transfer study of high speed flow over a spiked blunt body, *Int J Numerical Methods for Heat & Fluid Flow*, 2000, **10**, (7), pp 750 – 769.
18. KALIMUTHU, R., MEHTA, R.C. and RATHAKRISHANN, E. Blunt body drag reduction using aerospike and aerodisk at Mach 6, in the proceedings of International Conference on High Speed Trans-atmospheric Air & Space Transportation, Hyderabad, India, June 2007, pp 178 – 188.